

Accepted Manuscript

Identification of potent bovine viral diarrhea virus inhibitors by a structure-based virtual screening approach

Eliana F. Castro, Juan J. Casal, María J. España de Marco, Leandro Battini, Matías Fabiani, Gabriela A. Fernández, Ana M. Bruno, Lucía V. Cavallaro, Mariela Bollini

PII: S0960-894X(18)30918-1
DOI: <https://doi.org/10.1016/j.bmcl.2018.11.041>
Reference: BMCL 26152

To appear in: *Bioorganic & Medicinal Chemistry Letters*

Received Date: 20 August 2018
Revised Date: 8 November 2018
Accepted Date: 21 November 2018

Please cite this article as: Castro, E.F., Casal, J.J., de Marco, J.E., Battini, L., Fabiani, M., Fernández, G.A., Bruno, A.M., Cavallaro, L.V., Bollini, M., Identification of potent bovine viral diarrhea virus inhibitors by a structure-based virtual screening approach, *Bioorganic & Medicinal Chemistry Letters* (2018), doi: <https://doi.org/10.1016/j.bmcl.2018.11.041>

This is a PDF file of an unedited manuscript that has been accepted for publication. As a service to our customers we are providing this early version of the manuscript. The manuscript will undergo copyediting, typesetting, and review of the resulting proof before it is published in its final form. Please note that during the production process errors may be discovered which could affect the content, and all legal disclaimers that apply to the journal pertain.



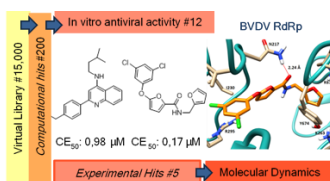
Graphical Abstract

To create your abstract, type over the instructions in the template box below.
Fonts or abstract dimensions should not be changed or altered.

Identification of potent bovine viral diarrhea virus inhibitors by a structure-based virtual screening approach

Leave this area blank for abstract info.

Eliana F. Castro^{a,&}, Juan J. Casal^{b,&}, María J. España de Marco^c, Leandro Battini^b, Matías Fabiani^a, Gabriela A. Fernández^b, Ana M. Bruno^d, Lucía V. Cavallaro^{c,*#}, Mariela Bollini^{b,*#}.





ELSEVIER

Bioorganic & Medicinal Chemistry Letters

journal homepage: www.elsevier.com

Identification of potent bovine viral diarrhea virus inhibitors by a structure-based virtual screening approach

Eliana F. Castro^{a,&}, Juan J. Casal^{b,&}, María J. España de Marco^c, Leandro Battini^b, Matías Fabiani^a, Gabriela A. Fernández^b, Ana M. Bruno^d, Lucía V. Cavallaro^{c,*#}, Mariela Bollini^{b,*#}.

^aCátedra de Virología, Departamento de Microbiología, Inmunología y Biotecnología, Consejo Nacional de Investigaciones Científicas y Técnicas, Facultad de Farmacia y Bioquímica, Universidad de Buenos Aires, Junín 956, 1113, Ciudad Autónoma de Buenos Aires, Argentina.

^bLaboratorio de Química Medicinal, Centro de Investigaciones en Bionanociencias (CIBION)-CONICET, Ciudad de Buenos Aires, Argentina.

^cCátedra de Virología, Departamento de Microbiología, Inmunología y Biotecnología, Facultad de Farmacia y Bioquímica, Universidad de Buenos Aires, Junín 956, 1113, Ciudad Autónoma de Buenos Aires, Argentina.

^dUniversidad de Buenos Aires, Facultad de Farmacia y Bioquímica, Departamento de Química Orgánica, Junín 956, C1113AAD, Ciudad Autónoma de Buenos Aires, Argentina.

ARTICLE INFO

ABSTRACT

Article history:

Received

Revised

Accepted

Available online

Keywords:

Keyword_1 BVDV inhibitors

Keyword_2 virtual screening,

Keyword_3 molecular dynamic simulation,

Keyword_4 RdRp protein

Keyword_5 antiviral

Bovine viral diarrhea virus (BVDV) is a pestivirus whose infection in cattle is globally distributed. The use of antivirals could complement vaccination as a tool of control and reduce economic losses. The RNA-dependent RNA polymerase (RdRp) of the virus is essential for its genome replication and constitutes an attractive target for the identification of antivirals. With the aim of obtaining selective BVDV inhibitors, the crystal structure of BVDV RdRp was used to perform a virtual screening. Approximately 15,000 small molecules from commercial and in-house databases were evaluated and several structurally different compounds were tested in vitro for antiviral activity. Interestingly, of twelve evaluated compounds, five were active and displayed EC₅₀ values in the sub and low-micromolar range. Time of drug addition experiment and measured intracellular BVDV RNA showed that compound **7** act during RNA synthesis. Molecular Dynamics and MM/PBSA calculation were done to characterize the interaction of the most active compounds with RdRp, which will allow future ligand optimization. These studies highlight the use of in silico screening to identify a new class of BVDV inhibitors.

2009 Elsevier Ltd. All rights reserved.

Bovine viral diarrhea virus 1 (BVDV), named Pestivirus A from 2017 International Committee on Taxonomy of Viruses report belongs to the *Pestivirus* genus of the family *Flaviviridae*. ¹BVDV infection is globally distributed being endemic in many countries.^{2,3} The latest data reported for Argentina showed a prevalence of anti-BVDV antibodies in 70% adult cattle. ⁴BVDV infections can manifest as generalized immunosuppression (leading to co-infections), fertility difficulties both in male and female cattle, and other variable signs such as fever, diarrhea and respiratory dysfunction.⁵⁻⁸ This leads to considerable financial losses within the livestock industry because of lower reproductive accomplishment, lower weight gain, reduced milk production, increased mortality, early slaughter as well as increased expenditures for veterinary services.⁹

The control of BVDV infections combines vaccination, which is not mandatory in some countries, with the detection and removal of persistently infected animals. The vaccination strategy has a disadvantage in terms of the time it takes to activate the animal's immune response and the increase in the antibody titer needed to protect against an infection. That is why the need to have effective and rapid control tools is considered, and the use of antivirals could be useful for this purpose.

The viral genome consists of a single-stranded (+) RNA which constitutes a unique open reading frame (ORF) that is flanked by 5' and 3' nontranslated regions (NTRs). This ORF encodes a 3,900 amino acids long polyprotein that is co- and post-translationally processed to the mature viral proteins by cellular and viral proteases. From its N-terminal, the ORF encodes the viral nonstructural protein (NS) Npro, the structural proteins (capsid protein C, the glycoprotein Erns, and the envelope glycoproteins E1 and E2) and the rest of the NS proteins: p7, NS2-3 (NS2, NS3), NS4A, NS4B, NS5A and NS5B. The last protein, is the viral RNA-dependent RNA polymerase (RdRp).¹⁰

As shown by its crystal structure, the RdRp of BVDV has the shape of a right hand that is divided into different domains: fingers, palm and thumb. The inner surfaces of these three domains form a central template-binding channel; and the N-terminal portion of and a long insert in the fingers domain (residues 71-138 and 260-288, respectively) form the fingertip region.^{11,12}

The fingertips, associated with the thumb domain, forms the entrance to the template-binding channel. It was also reported that the fingertip region is involved in template/product translocation, dimerization of the RdRp and other protein-protein interactions that enable the assembly of an active replication complex.^{11,12} Moreover, motifs I and II, which are involved in

RNA template and NTP binding in the RNA polymerases, were located within this region.¹²

Different selective antiviral agents against BVDV select resistant virus that carry mutations within the fingertip region. Previously, we described the antiviral mechanism of action of Thiosemicabazones derived from 1-indanones (TSC), which selected two specific mutations within NS5B: N264 and A392.¹³ Both mutations are located near F224, a residue that was mutated in BVDV-resistant mutants selected with other non-nucleoside inhibitors (NNIs) for BVDV, such as BPIP,¹⁴ VP32947,¹⁵ and LZ37.¹⁶ The cavity where these compounds bind represents one allosteric site of inhibition for BVDV RdRp, whose hydrophobicity complements the lipophilicity of TSC¹³ and of the other NNIs.

Computer-aided drug design (CADD) becomes increasingly important in drug research and development. CADD contributed, among other applications, to efficient data analysis, to the filtering of collections of compounds to select molecules for experimental evaluation, and to the generation of hypotheses to understand the mechanism of action of drugs and the design of novel chemical structures.^{17–20} In this work, we have employed a multistep High throughput docking (HTD) screening strategy to find novel viral polymerase inhibitors using synthetic druglike compounds (from our in-house library) and commercially available chemical libraries, and the crystal structure of the BVDV RdRp (1S48).¹² Design was targeted against the RdRp allosteric site of inhibition described for other NNIs (as described above). The original ~15,000 compounds collection was filtered based on known toxicophores and physicochemical properties.^{17,20,21} After removing metal atoms, duplicates, multiple fragments and more than one stereocenter we obtained a database of 13,000 in-stock compounds which were subjected to two independent HTD. The top 1,000 structures were redocked with Autodock Vina²² increasing the exhaustiveness to 25. The 200 ranked compounds were inspected by eye to assess scaffold diversity, and synthetic feasibility for further modifications. Finally, twelve compounds were synthesized (Scheme S1) or purchased for further *in vitro* study (Figure S1).

First, we assayed selected compounds for cytotoxicity. Cytotoxic concentration 50 (CC₅₀) is defined as the concentration of compound that reduces by 50% cell culture viability and maximum non-cytotoxic concentration (MNCC) was the higher concentration of compound evaluated that did not result cytotoxic in MDBK cells. Then, their antiviral activity (EC₅₀: concentration of compound that reduces viral cytopathic effect by 50%) against BVDV in cultured MDBK cells was studied. Selectivity Indexes

(SI) were determined as the ratio between CC₅₀ and EC₅₀. Compound **3** displayed high cytotoxicity (CC₅₀=2.11 μM) and was evaluated to its MNCC. The evaluation of all computational hits (Table 1) yielded five active compounds (Figure 1). Compounds **1** and **9** showed moderate micromolar activity with EC₅₀ values of 9.68 and 6.40 μM, respectively. Compound **10** displayed a promising antiviral activity, with EC₅₀ values of 2.30 μM. Finally, compounds **7** and **11** were the most active ones of this series, showing EC₅₀ values of 0.98 μM and 0.17 μM, respectively. Compound **11** displayed a wide window therapeutic index (SI=196.47) making this drug a suitable candidate for *in vivo* studies.

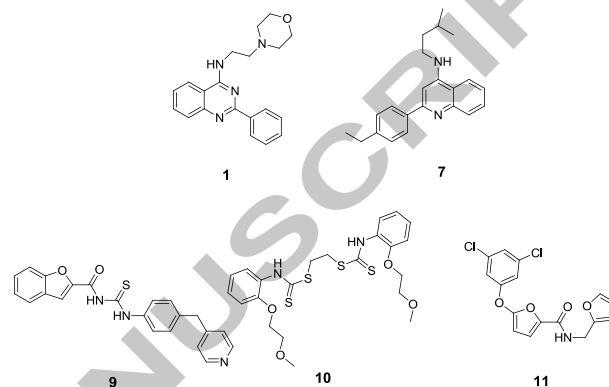


Figure 1. Active compounds against BVDV selected by virtual screening against viral RdRp.

We performed 60 ns MD simulation for each compound to evaluate the role of water molecules which were discarded during the molecular docking simulation, and to characterize the most likely interactions with the BVDV RdRp. For the MD simulation we started with the docked poses as initial conformation. Protein-ligand complexes were stable in each simulation (Figure S1). Additionally, to understand the forces involved in substrate binding, total binding free energy and individual energy components for each system were obtained by using the Molecular Mechanics Poisson–Boltzmann Surface Area (MM-PBSA) method based on the MD trajectories. The predicted binding free energies calculated for the most active compounds are more favorable than for inactive compounds. Active compounds **7** and **11** display ΔG_{bind} of -21.98 and -19.31 kcal/mol, respectively, while the ΔG_{bind} for inactive compounds **2** and **4** are -9.85 and -9.88 kcal/mol, respectively (For the rest of compounds see Table S1 in SI).

Table 1. In vitro cytotoxicity and anti-BVDV activity of selected compounds

Library	Compound	CC ₅₀ ± SD ^a (μM)	MNCC ^c (μM)	EC ₅₀ ± SD ^d (μM)	SI ^f
In-house Library	1	55.90 ± 8.20	12.50	9.68 ± 0.49	5.77
	2	UD ^b	6.00	Inactive ^e	-
	3	2.11 ± 0.01	0.78	Inactive	-
Maybridge HitFinder	4	>100	50.00	Inactive	-
	5	>100	25.00	Inactive	-
	6	>100.00	50.00	Inactive	-
	7	11.24 ± 2.86	3.13	0.98 ± 0.01	11.53
	8	>100.00	100.00	Inactive	-
	9	82.30 ± 13.20	25.00	6.40 ± 0.70	12.86
	10	43.06 ± 2.80	25.00	2.30 ± 0.70	18.72
	11	33.40 ± 0.50	6.25	0.17 ± 0.03	196.47
	12	34.30 ± 0.10	6.25	UD	UD

^aCC₅₀: compound concentration that reduces cell viability by 50%; ^bUD: undetermined; ^cMNCC: Maximum non-cytotoxic concentration; ^dEC₅₀: compound concentration that reduces viral CPE by 50%; ^eInactive: less than 50% of inhibition of CPE at MNCC; ^fSI: selectivity index (SI=CC₅₀/EC₅₀).

The predicted interaction of compound **7** with the hydrophobic cleft of RdRp is shown in Figure 2 A. This ligand presented hydrogen bond between the NH of the 4-aminoquinoline and the carbonyl O atom of the G406 with an average distance of 2.4 Å until 1.7 ns of simulation. While this hydrogen bond is broken, the ligand moves slightly from the initial conformation to another conformation that remains stable during the rest of the simulation, and a new hydrogen bond is formed between the N atom of the 4-aminoquinoline and a NH group of R295. The interatomic distance and angle that characterize the hydrogen bond are closer to 2 Å and 160° (Figure S3A). Additionally, the system was mostly stabilized by hydrophobic contacts, with extensive interactions being established with V216, I230, T299, P408 and L296. This is in agreement with the results obtained by MM-PBSA calculations, in which the VDW term is the main energy contribution (Table 2), highlighting the complementarity between the ligand and the binding pocket. Furthermore, the observations of the MD trajectory coincide with the per residue energy decomposition analysis (Figure 4), as the residue with the larger enthalpy contribution is R295, followed by V216 and I230. A stable cation- π interaction was observed between the aromatic ring of quinazoline and K307 throughout the simulation: the a N⁺-ring centroid distance is below 6 Å, and an acceptable θ angle of $\sim 40^\circ$ is maintained at all times during the simulation. (Figure S4).²³

As shown in Table 2, the VDW energy contribution is also predominant for compound **11**. In this sense, the docked complex does not present hydrogen-bond type interactions, instead, the predicted pose is stabilized by multiple hydrophobic interactions with the surrounding amino acids (N217, I230, V216, A221 and

I261). The interactions with N217, I230 and V216 were kept during the MD simulation, but the contacts with A221 and I261 disappeared due to the movement of the furan fragment of the ligands away from these amino acids. Moreover, a weak hydrogen bond is formed during the simulation, involving the oxygen of the phenyl ether of **11** and the NH₂ of N217, with interatomic distances and angles closer to 2.7 Å and 120°, respectively (Figure 2, S2B). Additionally, close contacts are seen in the last 30 ns of the simulation between the furan and the residues Y674 and K672 (Figure 3). This interaction correlates with the establishment of a stable conformation of the ligand (Figure S2B) and it is enabled because of the movement of the C-terminal region of RdRp during the simulation, which brings Y674 closer to the binding pocket. These observations are consistent with the per residue energy decomposition analysis of the MM-PBSA calculations (Figure 4), in which the amino acids with the larger energy contribution are N217 and Y674.

Overall, molecular dynamics simulations revealed the interaction of the active compounds with the allosteric site. It is important to highlight that these new compounds would interact with amino acids different from those reported for the majority of BVDV NNIs, which includes F224, N264, I390 and A392.¹³⁻¹⁶ In this work, the computational model shows the importance of the interactions with Y674, R295 and N217. These three polymerase residues were reported to interact with arylazoamine derivatives,²⁴ and both R295 and Y674 were also reported to be important for pyridoquinoxalines binding²⁵ to BVDV RdRp.

Table 2. Predicted free energies for binding of **7** and **11** to RdRp by MM-PBSA binding free energies method.

Compound	ΔE_{vdw}	ΔE_{ELE}	ΔG_{PB}	ΔG_{NPB}	ΔG_{bind}
7	-38.18 \pm 0.42	-7.84 \pm 0.39	28.32 \pm 0.52	-4.28 \pm 0.03	-21.98 \pm 0.62
11	-36.21 \pm 0.64	-1.53 \pm 0.36	22.52 \pm 0.72	-4.10 \pm 0.05	-19.31 \pm 0.61

All energies are expressed in kcal/mol. Data are mean values \pm SD. ΔE_{vdw} , van der Waals energy; ΔE_{ELE} , electrostatic energy; ΔG_{PB} , polar solvation energy; ΔG_{NPB} , nonpolar solvation energy; ΔG_{bind} , binding free energy, $-\Delta TS$, entropy contribution was not considered.

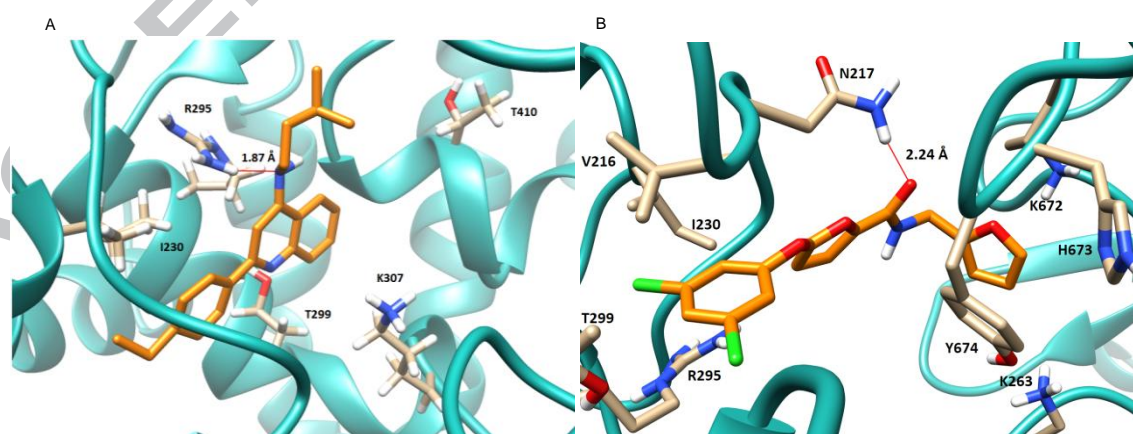


Figure 2. Predicted interaction of active compounds **7** (A) and **11** (B) within the RdRp (PDB ID 1S48) protein binding site, extracted from the molecular dynamics simulations. Color code: ligand carbons, orange; protein carbons, cyan; oxygens, red; nitrogens, blue; polar hydrogens, white; chlorine, green. Figure prepared with UCSF Chimera 1.13.²⁶

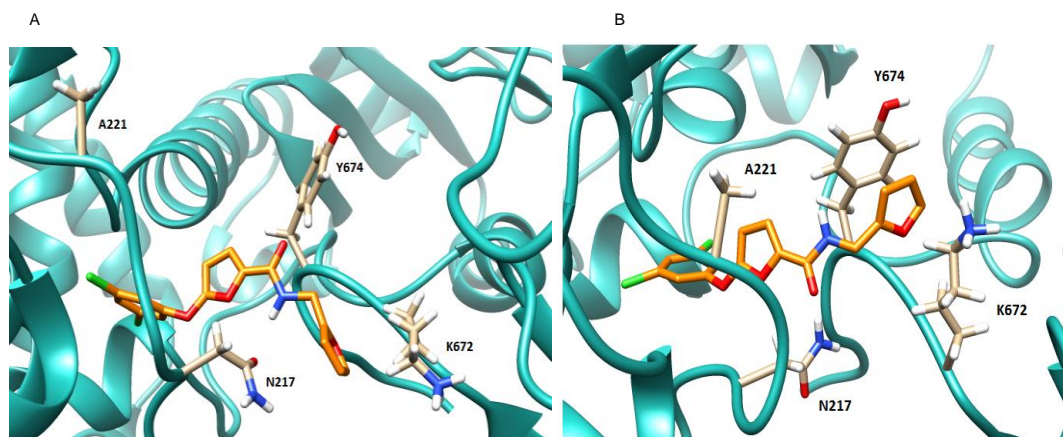


Figure 3. Predicted interaction of compound **11** within the RdRp (PDB ID 1S48) protein binding site, extracted from the molecular dynamics simulations. (A) First 30 ns simulation, (B) last 30 ns simulation. Color code: ligand carbons, orange; protein carbons, cyan; oxygens, red; nitrogens, blue; polar hydrogens, white; chlorine, green. Figure prepared with UCSF Chimera 1.13.²⁶

The BVDV RdRp structure reveals the shape of a right hand composed of the fingers, palm and thumb domains. According to RdRp structure,¹² both R295 and N217 locate in the fingers domain. During viral RNA synthesis, the phosphate backbone of the template interacts with residues mainly from this domain. Interestingly, R295 is part of the motif II of the polymerase, which is conserved between different RNA polymerases of positive RNA viruses.^{12,27} In addition, it was reported that substitution at this residue completely abolished RNA synthesis.^{25,27}

On the other hand, Y674 is located within the C-terminal loop in the thumb domain. The β -thumb region interacts with the fingers and palm domains through this long C-terminal loop (residues 670–679). Together with a loop between α -20 and α -21 in the thumb domain, the β -thumb reduces the volume of the template channel, and the C-terminal loop, in combination with the fingertip region, facilitates the translocation of the template and product RNA.¹²

Therefore, the amino acids with which compound **7** and **11** would interact would participate in essential processes during viral RNA synthesis.

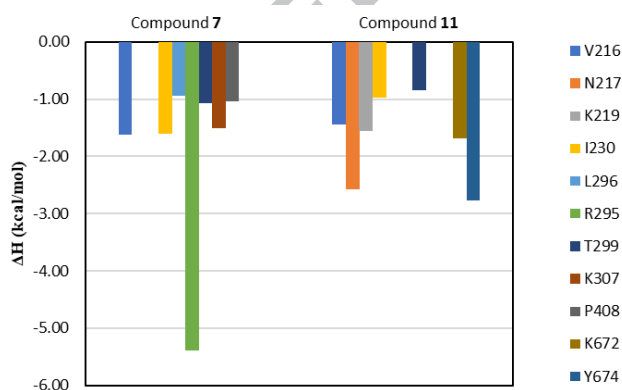


Figure 4. Per-residue calculated binding enthalpy decomposition ΔH , for compounds **7** and **11** in complex with BVDV RdRp

To get insight into the mechanism of action, we selected one of the most active compounds (**7**) and evaluated its effect on viral RNA synthesis. For that purpose, we performed a time of drug addition experiment and measured intracellular BVDV RNA (ivRNA) at 12h post adsorption (p.a.) (Figure 5). Results showed that when compound **7** was added during the first 8 h p.a. ivRNA production is reduced. There was a gradual loss of inhibition between 6 and 8 h p.a. and the addition at later time points (10 h p.a.) led to ivRNA levels similar to that observed in infected cells

not treated with the compound (UTC). This may indicate that compound **7** would act between 6 and 8 h p.a. Previous reports showed that when BVDV infects MDBK cells, an increase in ivRNA occurs between 6 and 10 h p.a, suggesting that at that point of time occurs viral RNA synthesis.²⁸ Taken together, and in accordance with other non-nucleoside inhibitors of BVDV polymerase^{13,14,16,28}, compound **7** may act during BVDV RNA synthesis.

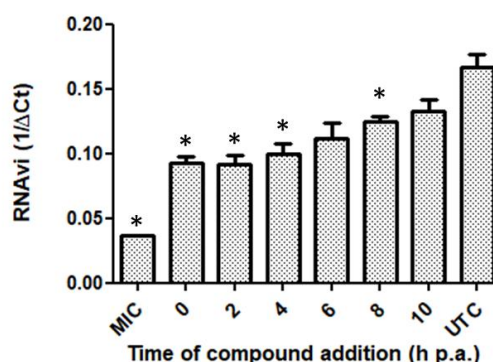


Figure 5. Effect of compound **7** addition on viral RNA synthesis. MDBK cells were infected with BVDV (MOI of 1), and 3.13 μ M of compound **7** was added every 2 h during the first 10 hours post-adsorption (h p.a.) The incubation period continued until 12 h p.a., when intracellular RNA was extracted and ivRNA measured by real-time PCR. A mock-infected control (MIC) and an infected untreated control (UTC) were included. Values are expressed as $1/\Delta CT$, where $\Delta CT = CT_{BVDV\ 5'NTR} - CT_{\beta\text{-actin}}$ endogenous control. *p value < 0.05 vs UTC.

In conclusion, we identified potential molecules that dock into the allosteric binding pocket of BVDV RdRp via structure-based virtual screening approach. Twelve compounds were synthesized or purchased and evaluated in a cell-based assay for cytotoxicity and antiviral activities. Interestingly, five of the compounds were active and displayed EC_{50} values in the sub and low-micromolar range. Molecular dynamics studies and free energy calculation were conducted to determine the key binding interactions between the most active compound and the residues into the RdRp binding site. Preliminary in vitro tests of the mechanism of antiviral action of compound **7** reinforced its potential as inhibitor of BVDV RdRp. Overall, these findings provide the basis to design a novel and improved BVDV antiviral.

ASSOCIATED CONTENT

Supporting Information. The Supporting Information is available free of charge at DOI: xxx Figures S1–S5, biological assay and organic synthesis.

AUTHOR INFORMATION

Corresponding Author

*Mariela Bollini, Phone: (+5411) 4899-5500 int 5622. E-mail mariela.bollini@cibion.conicet.gov.ar, *Lucia V. Cavallaro, Phone: (+5411) 5287-4474. E-mail lcavalla@ffy.uba.ar

Funding Sources

This work was supported by the Agencia Nacional de Promoción Científica y Tecnológica, Argentina (PICT 2013-0078, PICT 2014-1884, CONICET (PIP 2014 11220130100721 to MB), (PICT 2012-2867 and UBACYT 2014-2017 20920160100170BA to LVC).

Notes

The authors declare no competing financial interest.

Acknowledgments

Authors thank the TUPAC Cluster from CSC-CONICET, which is part of SNCAD-MinCyT, for granting use of their computational resources.

References

- Smith, D. B.; Meyers, G.; Bukh, J.; Gould, E. A.; Monath, T.; Scott Muerhoff, A.; Pletnev, A.; Rico-Hesse, R.; Stapleton, J. T.; Simmonds, P.; Becher, P. *J. Gen. Virol.* **2017**, *98*, 2106–2112.
- Baker, J. C. *Vet. Clin. North Am. Food Anim. Pract.* **1995**, *11*, 425–445.
- Chimeno Zoth, S.; Taboga, O. *J. Virol. Methods* **2006**, *138*, 99–108.
- Pacheco, J. M.; Lager, I. *Rev. Argent. Microbiol.* **2003**, *35*, 19–23.
- Fulton, R. W.; Purdy, C. W.; Confer, A. W.; Saliki, J. T.; Loan, R. W.; Briggs, R. E.; Burge, L. J. *Can. J. Vet. Res.* **2000**, *64*, 151–9.
- Fray, M. ; Paton, D. ; Alenius, S. *Anim. Reprod. Sci.* **2000**, *60–61*, 615–627.
- Hessman, B. E.; Fulton, R. W.; Sjeklocha, D. B.; Murphy, T. A.; Ridpath, J. F.; Payton, M. E. *Am. J. Vet. Res.* **2009**, *70*, 73–85.
- Beaudeau, F.; Fourichon, C.; Robert, A.; Joly, A.; Seegers, H. *Prev. Vet. Med.* **2005**, *72*, 163–167.
- Houe, H. *Biologicals* **2003**, *31*, 137–43.
- Lindenbach, B. D.; Heinz-Jürgen, T.; Rice, C. M. In *Fields virology*; Knipe, D. M.; et al, Eds.; Lippincott Williams & Wilkins: Philadelphia, PA, **2007**; pp. 1126–1131.
- Choi, K. H.; Gallei, A.; Becher, P.; Rossmann, M. G. *Structure* **2006**, *14*, 1107–13.
- Choi, K. H.; Groarke, J. M.; Young, D. C.; Kuhn, R. J.; Smith, J. L.; Pevear, D. C.; Rossmann, M. G. *Proc. Natl. Acad. Sci.* **2004**, *101*, 4425–4430.
- Castro, E. F.; Fabian, L. E.; Caputto, M. E.; Gagey, D.; Finkielstein, L. M.; Moltrasio, G. Y.; Moglioni, A. G.; Campos, R. H.; Cavallaro, L. V. *J. Virol.* **2011**, *85*, 5436–5445.
- Paeshuyse, J.; Chezal, J.-M.; Froeyen, M.; Leyssen, P.; Dutartre, H.; Vrancken, R.; Canard, B.; Letellier, C.; Li, T.; Mittendorfer, H.; Koenen, F.; Kerkhofs, P.; De Clercq, E.; Herdewijn, P.; Puerstinger, G.; Gueffier, A.; Chavignon, O.; Teulade, J.-C.; Neyts, J. *J. Virol.* **2007**, *81*, 11046–11053.
- Baginski, S. G.; Pevear, D. C.; Seipel, M.; Sun, S. C. C.; Benetatos, C. A.; Chunduru, S. K.; Rice, C. M.; Collett, M. S. *Proc. Natl. Acad. Sci.* **2000**, *97*, 7981–7986.
- Paeshuyse, J.; Letellier, C.; Froeyen, M.; Dutartre, H.; Vrancken, R.; Canard, B.; De Clercq, E.; Gueffier, A.; Teulade, J.-C.; Herdewijn, P.; Puerstinger, G.; Koenen, F.; Kerkhofs, P.; Baraldi, P. G.; Neyts, J. *Antiviral Res.* **2009**, *82*, 141–7.
- Bollini, M.; Leal, E. S.; Adler, N. S.; Aucar, M. G.; Fernández, G. A.; Pascual, M. J.; Merwaiss, F.; Alvarez, D. E.; Cavasotto, C. N. *Front. Chem.* **2018**, *6*, 79.
- Nichols, S. E.; Domaal, R. A.; Thakur, V. V.; Tirado-rives, J.; Anderson, K. S.; Jorgensen, W. L. **2009**, 1272–1279.
- Leal, E. S.; Aucar, M. G.; Gebhard, L. G.; Iglesias, N. G.; Pascual, M. J.; Casal, J. J.; Gamarnik, A. V.; Cavasotto, C. N.; Bollini, M. *Bioorg. Med. Chem. Lett.* **2017**, *27*, 3851–3855.
- Pascual, M. J.; Merwaiss, F.; Leal, E.; Quintana, M. E.; Capozzo, A. V.; Cavasotto, C. N.; Bollini, M.; Alvarez, D. E. *Antiviral Res.* **2018**, *149*, 179–190.
- Leal, E. S.; Aucar, M. G.; Gebhard, L. G.; Iglesias, N. G.; Pascual, M. J.; Casal, J. J.; Gamarnik, A. V.; Cavasotto, C. N.; Bollini, M. *Bioorg. Med. Chem. Lett.* **2017**, *27*, 3851–3855.
- Trott, O.; Olson, A. J. *J. Comput. Chem.* **2010**, *31*, 455–461.
- Marshall, M. S.; Steele, R. P.; Thanthirawatte, K. S.; Sherrill, C. D. *J. Phys. Chem. A* **2009**, *113*, 13628–13632.
- Giliberti, G.; Ibba, C.; Marongiu, E.; Loddo, R.; Tonelli, M.; Boido, V.; Laurini, E.; Posocco, P.; Fermeglia, M.; Pricl, S. *Bioorg. Med. Chem.* **2010**, *18*, 6055–6068.
- Carta, A.; Briguglio, I.; Piras, S.; Corona, P.; Ibba, R.; Laurini, E.; Fermeglia, M.; Pricl, S.; Desideri, N.; Atzori, E. M.; La Colla, P.; Collu, G.; Delogu, I.; Loddo, R. *Eur. J. Med. Chem.* **2016**, *117*, 321–334.
- Pettersen, E. F.; Goddard, T. D.; Huang, C. C.; Couch, G. S.; Greenblatt, D. M.; Meng, E. C.; Ferrin, T. E. *J. Comput. Chem.* **2004**, *25*, 1605–1612.
- Lai, V. C.; Kao, C. C.; Ferrari, E.; Park, J.; Uss, A. S.; Wright-Minogue, J.; Hong, Z.; Lau, J. Y. *J. Virol.* **1999**, *73*, 10129–36.
- Paeshuyse, J.; Leyssen, P.; Mabery, E.; Boddeker, N.; Vrancken, R.; Froeyen, M.; Ansari, I. H.; Dutartre, H.; Rozenki, J.; Gil, L. H. V. G.; Letellier, C.; Lanford, R.; Canard, B.; Koenen, F.; Kerkhofs, P.; Donis, R. O.; Herdewijn, P.; Watson, J.; De Clercq, E.; Puerstinger, G.; Neyts, J. *J. Virol.* **2006**, *80*, 149–160.

*Highlights

- Docking based virtual screening was used to identify new inhibitors of BVDV RdRp
- Five compounds displayed excellent potency against BVDV
- Molecular dynamics were carried out to identify key RdRp-ligand interactions
- In vitro experiments showed that compound 7 may act during BVDV RNA synthesis

ACCEPTED MANUSCRIPT